Synergistic interactions promote behavior spreading and alter phase transitions on multiplex networks

Quan-Hui Liu,[1,2,3] Wei Wang,[1,2,4] Shi-Min Cai,[1,2,5] Ming Tang,[1,2,6,*] and Ying-Cheng Lai[7]

[1]*Web Sciences Center, School of Computer Science and Engineering, University of Electronic Science and Technology of China, Chengdu 611731, China*

[2]*Big Data Research Center, University of Electronic Science and Technology of China, Chengdu 611731, China*

[3]*Laboratory for the Modeling of Biological and Socio-technical Systems, Northeastern University, Boston, Massachusetts 02115, USA*

[4]*College of Computer Science and Technology, Chongqing University of Posts and Telecommunications, Chongqing 400065, China*

[5]*Center for Polymer Studies and Department of Physics, Boston University, Boston, Massachusetts 02215, USA*

[6]*School of Information Science Technology, East China Normal University, Shanghai 200241, China*

[7]*School of Electrical, Computer and Energy Engineering, Arizona State University, Tempe, Arizona 85287, USA*

(Received 5 October 2017; published 21 February 2018)

Synergistic interactions are ubiquitous in the real world. Recent studies have revealed that, for a single-layer network, synergy can enhance spreading and even induce an explosive contagion. There is at the present a growing interest in behavior spreading dynamics on multiplex networks. What is the role of synergistic interactions in behavior spreading in such networked systems? To address this question, we articulate a synergistic behavior spreading model on a double layer network, where the key manifestation of the synergistic interactions is that the adoption of one behavior by a node in one layer enhances its probability of adopting the behavior in the other layer. A general result is that synergistic interactions can greatly enhance the spreading of the behaviors in both layers. A remarkable phenomenon is that the interactions can alter the nature of the phase transition associated with behavior adoption or spreading dynamics. In particular, depending on the transmission rate of one behavior in a network layer, synergistic interactions can lead to a discontinuous (first-order) or a continuous (second-order) transition in the adoption scope of the other behavior with respect to its transmission rate. A surprising two-stage spreading process can arise: due to synergy, nodes having adopted one behavior in one layer adopt the other behavior in the other layer and then prompt the remaining nodes in this layer to quickly adopt the behavior. Analytically, we develop an edge-based compartmental theory and perform a bifurcation analysis to fully understand, in the weak synergistic interaction regime where the dynamical correlation between the network layers is negligible, the role of the interactions in promoting the social behavioral spreading dynamics in the whole system.

DOI: 10.1103/PhysRevE.97.022311

I. INTRODUCTION

A central problem in network science and engineering is to understand, predict, and control the dynamics of virus or information spreading on complex networks [1–3]. Social contagion processes such as the propagation of an opinion, diffusion of a belief, and spread of a particular behavior occur commonly in the real world [4–11]. With the modern technological advances, a variety of online social networking platforms (e.g., *Facebook* and *YouTube*) have become a routine necessity for a substantial fraction of individuals in the entire population. Spreading dynamics in modern online social networks have attracted a great deal of recent attention and a variety of mathematical models have been articulated to understand and predict the relevant phenomena [3,12–14]. For example, the threshold model, a binary state spreading model, was introduced earlier to address the phenomenon of behavior adoption, where a node in a social network adopts a new behavior only when the number [15] or the fraction [16] of its nearest adopted neighbors exceeds a threshold value. A representative threshold model reveals the phenomenon that the final size of the nodes adopting the behavior first grows continuously and then decreases discontinuously as the mean degree of the network is increased [16]. Within the threshold model, the effects of parameters and network structure on the dynamics of social behavioral spreading have been studied, which include the initial seed size [17], the clustering coefficient [18–20], the community structure [21,22], and multiplexity [23–25]. The dynamical process described by the threshold model, however, is Markovian because the state of a node depends only on the current state of its neighbors. The original model is thus not able to encompass an important aspect of real contagion dynamics: social reinforcement originated from the memory effect [26–29]—a feature that is characteristically non-Markovian. To overcome this deficiency of the classical threshold model, a non-Markovian behavior spreading model taking into account the received cumulative pieces of behavioral information for any node to adopt the behavior was introduced [30]. A prediction of the modified model is that the dependence of the final behavior adoption size on the information transmission rate can change from being

*tangminghan007@gmail.com

discontinuous to being continuous through continuous changes in the dynamical or structural parameters. The non-Markovian behavior spreading model also allows additional issues such as the heterogeneity of adoption thresholds [31], the limited contact capacity [32], and the effect of temporal network structure [33] to be addressed.

Most previous works on network behavior spreading focused on a single social behavior contagion process through empirical methods [8,9] and mathematical models [13–16,30,34]. In the real world, it is common for two or more distinct behaviors to spread simultaneously in a social system, where interactions between the corresponding spreading processes inevitably arise. For example, individuals who have adopted Windows services are more likely to use other services from the same company, e.g., Microsoft Office. In online networking systems, two different tweets on the same event or subject can diffuse on the twitter network at the same time. The user seeing one tweet will experience an increased exposure to the other tweet, and vice versa, since these two tweets are closely related. In this case, the two tweets spread synergistically as they mutually prompt each other in the process of retweeting [35]. The synergistic mechanism is also typical in the adoption of online services. A good example is the adoption of two online services, say Google and YouTube through two types of tweets: one containing the URLs with Google and another with YouTube. The numbers of the two types of tweets are synchronized most of the time, implying that they are synergistic to each other [36]. The synergistic effect also occurs in disease spreading, where the interaction between pathogens may mutually strengthen their spreading process, and such an effect may have played a role in the coepidemic of the Spanish flu and pneumonia in 1918 [37–41]. In spite of its ubiquity, the synergistic mechanism among two or more simultaneously spreading behaviors was not investigated in previous studies [13–16,30].

In this paper, we articulate a synergistic social behaviors spreading model to address and understand the impacts of synergistic interactions among multiple behaviors on their spreading. As the spreading of each behavior typically occurs on a different network layer, it is necessary to incorporate a multilayer network structure [42–44]. To be concrete, we consider the spreading dynamics of two distinct behaviors in two-layer coupled networks, where each layer supports the spreading of one behavior with its own transmission path, as described by a non-Markovian process. The synergistic mechanism between the two behavior adoption dynamics is that, once a node adopts a behavior in one layer, it becomes more susceptible to adopting the other behavior that spreads in the other network layer. We develop an edge-based compartmental theory to analyze and understand how the synergistic interactions impact the simultaneous spreading dynamics of the behaviors. We find, as suggested by intuition, that the synergistic interactions greatly facilitate the adoption of both behaviors. However, surprisingly, a phenomenon is that the adoption of one behavior can lead to a characteristic change in the adoption of the other behavior: its final adoption size versus its information rate can change from being discontinuous to continuous, where the former corresponds to a first-order phase transition while the latter corresponds to a second-order transition. Remarkably, the synergistic effect can induce a two-stage contagion process, in which nodes having adopted one behavior in one layer will adopt the other behavior in the other layer. When there is a sufficient number of seeds, i.e., when the number of nodes having adopted the other behavior in the other layer is sufficiently large, the remaining nodes will adopt the behavior quickly. While it is intuitively understandable that the synergistic interactions can promote the spreading dynamics of the distinct behaviors involved, our work lays a quantitative foundation for this phenomenon. Our model will not only serve as a useful framework to understand the interplay between synergy and simultaneous spreading of multiple behaviors or diseases, but will also provide insight into predicting or even controlling the underlying dynamics. Due to the ubiquity of synergy in different fields such as social science, computer science, biology, and biomedicine, broad relevance of our model is warranted.

In Sec. II, we describe the network and the synergistic behavior spreading models. In Sec. III, we carry out a detailed theoretical analysis. In Sec. IV, we present extensive simulation results with respect to the theoretical predictions. In Sec. V, we summarize the main results and discuss a few pertinent issues.

II. MODEL

There are two components in our model: multiplex networks and spreading dynamics of synergistic behaviors. We first introduce the model of multiplex networks, and then present the synergistic behavior spreading model.

A. Model of multiplex networks

In general, network layers in an interdependent networked system have different internal structures and dynamical functions. To capture the essential dynamics of simultaneous spreading of distinct behaviors, we focus on multiplex networks [42–44]. Consider the simple setting of a duplex system consisting of two layers or subnetworks. Initially, we generate two independent layers, denoted as a and b, which have the same node set and support the spread of behaviors 1 and 2, respectively. We use the configuration model [45] to generate each subnetwork, where the degree distribution $P_a(k_a)$ of layer a is completely independent of the distribution $P_b(k_b)$ of layer b. For large and sparse subnetworks, the configuration model stipulates that both interlayer and intralayer degree-degree correlations are negligible.

B. Synergistic behavior spreading model

We use a representative non-Markovian spreading model, the susceptible-adopted-recovered (SAR) [30] model, to describe the dynamics of behavior spreading, and then introduce the synergistic mechanism between the spreading processes of the two behaviors.

For each behavior $c \in \{1,2\}$, at any time a node will be in one of the three states: susceptible (S_c), adopted (A_c) and recovered (R_c). A node in state S_c has not adopted behavior c but it has an interest in c. A node in the A_c state has adopted the behavior and can transmit the information about the behavior (denoted as information c) to its neighbors. The node loses interest in transmitting the information when it is in the R_c

state. The evolution process of behavior c can be described, as follows. Initially, $\rho_c(0)$ fraction of nodes are randomly chosen as the nodes that have adopted the behavior and the remaining nodes are set to be in the susceptible state. At each time step, each node in the A_c state transmits the information to each of its susceptible neighbors with the transmission rate λ_c. Suppose a neighboring node v already has accumulated $m-1$ pieces of information c from its distinct neighbors. One more successful transmission will make the number of information pieces to become m. We assume nonredundant information transmission, i.e., once an adopted node has transmitted the information to node v, the former will not transmit the same information to the latter again. If the cumulative number m pieces of information c that the susceptible node v has is equal to or larger than a threshold, the node will adopt the behavior c and changes its state to A_c. Simultaneously, each A_c node will turn to the R_c state at the recovery rate γ_c. The behavior spreading process will terminate when all the adopted nodes have recovered. More specifically, $\rho_1(0)$ and $\rho_2(0)$ are the fractions of nodes randomly chosen as seeds (i.e., adopted nodes) for behavior 1 and 2 on each layer, respectively, where the remaining nodes are in the susceptible state. Information 1 (2) diffuses in layer a (b) with transmission rate λ_1 (λ_2), and the recovery rates for behaviors 1 and 2 are γ_1 and γ_2, respectively.

In the general SAR model, each susceptible node has its own adoption threshold for a behavior. However, for simplicity in modeling the synergistic interaction between the spreading of the two behaviors, we assume that all nodes have the same adoption threshold for each behavior: we denote the adoption threshold for behavior 1 in layer a as T_1 and that for behavior 2 in layer b as T_2. As a manifestation of mutual synergy, a node having adopted one behavior will become more susceptible to adopting the other behavior. To quantify the synergistic effect, we assume that, once node i has adopted behavior 1 (2), it will generate an increase $\Delta T_2 > 0$ ($\Delta T_1 > 0$) in the number of pieces of information about behavior 2 (1). The quantities ΔT_1 and ΔT_2 thus characterize the strength of the synergistic effect, and we have $\Delta T_1 \in [0, T_1]$ and $\Delta T_2 \in [0, T_2]$. For $\Delta T_1 = 0$, a node having adopted behavior 2 in layer b will not impact on its adoption of behavior 1 in layer a. Similarly, the adoption of behavior 1 will have no effect on adopting behavior 2 if $\Delta T_2 = 0$. If a node has adopted behavior 2, it will adopt behavior 1 only if $\Delta T_1 + m \geqslant T_1$, where m represents the number of cumulative pieces of behavioral information 1 in layer a that this node has received from distinct neighbors.

III. THEORY

We exploit the edge-based compartmental theory [30,46–48] to analyze the dynamical process of behavior spreading subject to synergistic interactions, under the assumption that each subnetwork is large and sparse with no internal degree-degree correlations. We also assume that the degree distribution of network a is completely independent of that of network b, so interlayer degree-degree correlation can be neglected too. The fraction of nodes in each state can be treated as a continuous variable. For each behavior $c \in \{1,2\}$, we denote $S_c(t)$, $A_c(t)$, and $R_c(t)$ as the fractions of nodes being in the susceptible, adopted, and recovered state, respectively, for behavior c in the corresponding layer at time t. During the spreading process, the susceptible nodes adopting behavior c decreases the value of $S_c(t)$ but leads to an increase in $A_c(t)$, and the recovery of the adopted nodes for behavior c decreases $A_c(t)$ but increases $R_c(t)$. Using these notations, the dynamical evolution equations for behavior c can be written as

$$\frac{dA_c(t)}{dt} = -\frac{dS_c(t)}{dt} - \gamma_c A_c(t) \tag{1}$$

and

$$\frac{dR_c(t)}{dt} = \gamma_c A_c(t). \tag{2}$$

For $t \to \infty$, the states of all individuals remain unchanged and $R_c(\infty)$ is the final adoption fraction of behavior c.

A. Edge-based compartmental theory

Despite that the spreading processes of behaviors 1 and 2 occur in different networks (a and b, respectively) and the dynamical parameters such as the information transmission rates (λ_1 and λ_2), the recovery rates (γ_1 and γ_2), and the adoption thresholds (T_1 and T_2) are different, the mathematical equations governing the underlying processes have identical forms. It thus suffices to derive the equations for behavior 1 spreading in layer a.

To solve Eqs. (1) and (2), we need to calculate the fraction of susceptible nodes for behavior 1 at time step t. First, for nodes of degree k_a in layer a, two cases can arise where the nodes do not adopt behavior 1: (1) These nodes have not adopted behavior 2 on layer b and the cumulative number of received pieces of information 1 in layer a is less than T_1, and (2) these nodes have already adopted behavior 2 in layer b, but the cumulative number of received pieces of information 1 in layer a is less than $T_1 - \Delta T_1$. Under the assumption that there is no dynamical correlation between the layers, we have that the fraction of susceptible nodes of degree k_a for behavior 1 at time t is given by

$$S_1(k_a,t) = S_2(t) \sum_{m=0}^{T_1-1} \phi_1(k_a,m,t) + [1 - S_2(t)] \sum_{m=0}^{T_1-1-\Delta T_1} \phi_1(k_a,m,t). \tag{3}$$

In Eq. (3), the first term on the right side is the probability that a node of degree k_a in layer a at time t does not adopt behavior 1. This term contains two parts that describe the following two situations, respectively: (1) the received cumulative number of pieces of information 1 is less than T_1 with probability $\sum_{m=0}^{T_1-1} \phi_1(k_a,m,t)$, and (2) with probability $S_2(t)$, a random node in layer b does not adopt behavior 2 at time t (i.e., a node in layer b does not adopt behavior 2 and is still in the susceptible state), where the quantity $\phi_1(k_a,m,t)$ is the probability for a node of degree k_a to have received m pieces of information 1 by time t in layer a. Combining the two parts, we find that the first term is identical to the second term in Eq. (3). Using the degree distribution of network a, we can express the fraction of susceptible nodes for behavior 1 as

$$S_1(t) = \sum_{k_a} P_a(k_a) S_1(k_a,t). \tag{4}$$

In Eq. (3), the quantity $\phi_1(k_a,m,t)$ can be expressed as

$$\phi_1(k_a,m,t) = [1-\rho_1(0)]B_{k_a,m}[\theta_1(t)], \tag{5}$$

where $B_{k,m}(w)$ denotes the binomial distribution $B_{k,m}(1-w)^m w^{k-m}$ and $\theta_1(t)$ is the probability that a random neighbor v of node u in layer a has not transmitted the behavioral information 1 to node u by time t. To take into account the dynamical correlations among the states of the adjacent nodes, we make use of the cavity theory [30,46–48] to analyze the quantity $\theta_1(t)$, where node u is in the cavity state so that it cannot transmit the behavioral information to its neighbors but it can receive the information from its neighbors.

To solve Eqs. (3) and (4), we need the value of $\theta_1(t)$ [the computation of $S_2(t)$ is the same as that of $S_1(t)$]. Noting that a random neighbor v of node u in layer a can be in one of the following three states: S_1, A_1, and R_1, we have that $\theta_1(t)$ is the sum of the probabilities that the neighbor v does not transmit information 1 to u when v is in the S_1, A_1, or R_1 state. We have

$$\theta_1(t) = \xi_1^S(t) + \xi_1^A(t) + \xi_1^R(t), \tag{6}$$

where $\xi_1^S(t)$ [$\xi_1^A(t)$ or $\xi_1^R(t)$] denotes the susceptible (adopted or recovered) neighbor v of u which has not transmitted information 1 to node u up to time t in layer a.

Suppose a random neighbor v of degree k_a' of node u is susceptible initially; node u cannot transmit information 1 to v since u is in the cavity state. Node v can only receive the information from its other $k_a'-1$ neighbors. The probability that node v has received m pieces of information 1 in layer a by time t is then

$$\tau_1(k_a',m,t) = B_{k_a'-1,m}[\theta_1(t)]. \tag{7}$$

Similar to Eq. (3), we have that the probability that the neighboring node v is still in the susceptible state for behavior 1 at time t is given by

$$\Phi_1[k_a',\theta_1(t),\theta_2(t)] = S_2(t)\sum_{m=0}^{T_1-1}\tau_1(k_a',m,t) + [1-S_2(t)]\sum_{m=0}^{T_1-1-\Delta T_1}\tau_1(k_a',m,t). \tag{8}$$

For uncorrelated networks, the probability for a random edge to connect a node of degree k_a' is $k_a'P(k_a')/\langle k_a\rangle$, where $\langle k_a\rangle$ is the average degree of network layer a. A neighboring node in the susceptible state cannot transmit the behavioral information. Thus, $\xi_1^S(t)$ is equal to the probability that the neighboring node is in the susceptible state, which is

$$\xi_1^S(t) = [1-\rho_1(0)]\frac{\sum_{k_a'}k_a'P(k_a')\Phi_1[k_a',\theta_1(t),\theta_2(t)]}{\langle k_a\rangle}. \tag{9}$$

If a random neighbor v is in the adopted state for behavior 1, success in information transmission from node v to node u will result in a decrease in $\theta_1(t)$. We thus have

$$\frac{d\theta_1(t)}{dt} = -\lambda_1\xi_1^A(t). \tag{10}$$

At the same time, once the adopted neighbor v has recovered before it can transmit information 1 to node u, there will be an increase in $\xi_1^R(t)$. (Note that here we use the synchronous updating rule, meaning that the transmission and recovery events happen consecutively in discrete time steps.) The increase in $\xi_1^R(t)$ contains two parts that describe the following two situations, respectively: (1) with probability $1-\lambda_1$, the neighboring node v has not transmitted information 1 to u, and (2) simultaneously, node v recovers with probability γ_1. Combining these two parts, we obtain the increment of $\xi_1^R(t)$ as

$$\frac{d\xi_1^R(t)}{dt} = \gamma_1(1-\lambda_1)\xi_1^A(t). \tag{11}$$

Combining Eqs. (10) and (11), we obtain an explicit expression for $\xi_1^R(t)$:

$$\xi_1^R(t) = \frac{\gamma_1[1-\theta_1(t)](1-\lambda_1)}{\lambda_1}. \tag{12}$$

Inserting Eqs. (9) and (12) into Eq. (6), we can write $\xi_1^A(t)$ as

$$\xi_1^A(t) = \theta_1(t) - \frac{\sum_{k_a}' k_a'P(k_a')\Phi_1[k_a',\theta_1(t),\theta_2(t)]}{\langle k_a\rangle} - \frac{\gamma_1[1-\theta_1(t)](1-\lambda_1)}{\lambda_1}. \tag{13}$$

Substituting Eq. (13) into Eq. (10), we get the time evolution of $\theta_1(t)$ as

$$\frac{d\theta_1(t)}{dt} = -\lambda_1\theta_1(t) + \gamma_1[1-\theta_1(t)](1-\lambda_1) + \lambda_1(1-\rho_1(0)) \times \frac{\sum_{k_a'}k_a'P(k_a')\Phi_1[k_a',\theta_1(t),\theta_2(t)]}{\langle k_a\rangle}. \tag{14}$$

Following a similar procedure, we can derive the expression of $\theta_2(t)$, the probability that a random neighbor v of node u in layer b has not transmitted the behavioral information 2 to node u by time t, and $S_2(k_b,t)$. We have

$$\frac{d\theta_2(t)}{dt} = -\lambda_2\theta_2(t) + \gamma_2[1-\theta_2(t)](1-\lambda_2) + \lambda_2(1-\rho_2(0)) \times \frac{\sum_{k_b'}k_b'P(k_b')\Phi_2[k_b',\theta_1(t),\theta_2(t)]}{\langle k_a\rangle} \tag{15}$$

and

$$S_2(k_b,t) = S_1(t)\sum_{m=0}^{T_2-1}\phi_2(k_b,m,t) + [1-S_1(t)]\sum_{m=0}^{T_2-1-\Delta T_2}\phi_2(k_b,m,t), \tag{16}$$

where the form of $\Phi_2[k_b',\theta_1(t),\theta_2(t)]$ in Eq. (15) is similar to $\Phi_1[k_a',\theta_1(t),\theta_2(t)]$, and $\phi_2(k_b,t)$ in Eq. (16) is similar to $\phi_1(k_a,t)$. It is thus not necessary to write down the expressions again. Using the degree distribution of network b, we have the fraction of susceptible nodes at time t in layer b as

$$S_2(t) = \sum_{k_b}P_b(k_b)S_2(k_b,t). \tag{17}$$

Iterating Eqs. (1)–(4) and (14)–(17), we can obtain the fractions of susceptible nodes at time t in both layers: $S_1(t)$ and $S_2(t)$. In addition, we can substitute $S_1(t)$ [$S_2(t)$] into

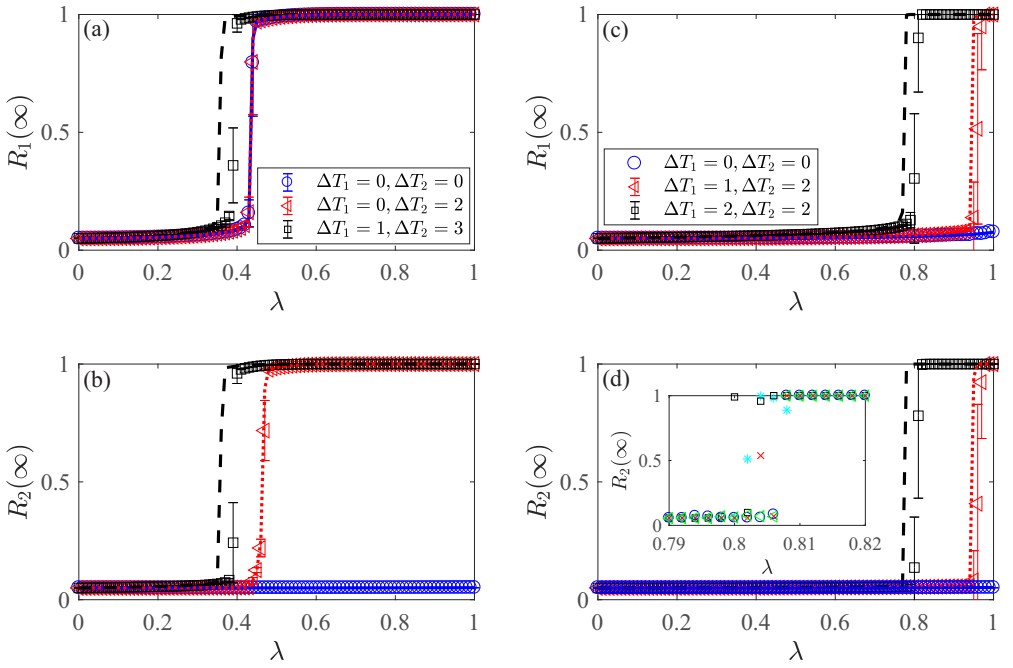

FIG. 1. Effect of synergistic strength on behavior spreading for random regular double-layer networks (RR-RR). (a),(b) For $T_1 = 2$ and $T_2 = 4$, the fractions $R_1(\infty)$ and $R_2(\infty)$ of recovered nodes in layers a and b, respectively, versus λ, where $\lambda_1 = \lambda_2 = \lambda$. (c),(d) The corresponding plots for a different set of threshold values: $T_1 = 3$ and $T_2 = 4$. The symbols are direct simulation results while the lines are the corresponding theoretical prediction obtained by iterating Eqs. (1)–(4) and (14)–(17). The plots in the inset of (d) are results from five stochastic simulations for the parameter settings ($\Delta T_1 = 2$, $\Delta T_2 = 2$, $T_1 = 3$, and $T_2 = 4$). The network sizes of both layers are set as $N = 5 \times 10^4$, the simulation results are averaged by using 20 multiplex network realizations, and each multiplex network is with 10^3 independent dynamical realizations. Other parameters are $\gamma_1 = \gamma_2 = 1$.

Eqs. (1) and (2) and calculate the fractions of the adopted nodes and of the recovered nodes in layer a (b) at time t. Taking the limit $t \to \infty$, we can obtain the final fractions of adoption of the two behaviors. Results on the final adoption fractions from direct numerical simulations together with the corresponding theoretical predictions for different parameter values are shown in Fig. 1. We obtain a good agreement between theory and numerics. For example, for $T_1 = 2$ and $T_2 = 4$, Fig. 1(b) shows that, without the synergistic effect of behavior 1, i.e., $\Delta T_2 = 0$, behavior 2 will not exhibit any outbreak. For $\Delta T_2 = 2$, behavior 2 is adopted globally. When there are mutual synergistic effects, e.g., $\Delta T_1 = 1$ and $\Delta T_2 = 3$ or $T_1 = 3$ and $T_2 = 4$, the adoption of both behaviors is enhanced, as shown in Figs. 1(c) and 1(d), respectively. Note that there are some outliers [e.g., there are is black square in Fig. 1(a) and two black squares in Fig. 1(d)] around the critical transmission rate since the SAR model is not a deterministic threshold model, which is in contrast to the Watts threshold model. The randomness exists in the process of simulations when the behavior information transmission rate is smaller than 1. Supposing a susceptible node with adoption threshold equal to 3, when it has three adopted neighbors it will not adopt the behavior if one of its adopted neighbors does not succeed in transmitting the behavior information. As shown in the inset of Fig. 1(d), there are some stochastic simulations that $R_2(\infty)$ does not jump from a small value (i.e., the value close to the initial fraction of adopted nodes) to 1 directly. Instead, $R_2(\infty)$ will jump to a value close to 0.5 first, and then increases to 1.

A fundamental issue in spreading dynamics in complex networks is phase transitions [3]. As a system parameter (e.g., the infection rate) changes through a critical point, the final size of the infected nodes starts to increase from zero. An abrupt and discontinuous increase in the final size signifies a first-order phase transition, while a gradual and continuous change is indicative of a second-order phase transition. An objective of our study is then to uncover and understand the effect of synergistic interactions on the phase transitions associated with the social behavior spreading dynamics. To analyze the phase transition, we focus on the fixed point (root) of Eqs. (14) and (15) associated with the final state (i.e., $t \to \infty$). Simplifying notation as $\theta_1 \equiv \theta_1(\infty)$ and $\theta_2 \equiv \theta_2(\infty)$, we write Eqs. (14) and (15) as

$$\theta_1 = f_1(\theta_1, \theta_2), \tag{18}$$

and

$$\theta_2 = f_2(\theta_1, \theta_2), \tag{19}$$

respectively, where

$$f_1(\theta_1, \theta_2) = \frac{[1 - \rho_1(0)] \sum_{k'_a} k'_a P_a(k'_a) \Phi_1(k'_a, \theta_1, \theta_2)}{\langle k_a \rangle} + \frac{\gamma_1}{\lambda_1}[1 - \theta_1](1 - \lambda_1), \tag{20}$$

and

$$f_2(\theta_1, \theta_2) = \frac{[1 - \rho_2(0)] \sum_{k'_b} k'_b P_b(k'_b) \Phi_2(k'_b, \theta_1, \theta_2)}{\langle k_b \rangle} + \frac{\gamma_2}{\lambda_2}[1 - \theta_2](1 - \lambda_2). \tag{21}$$

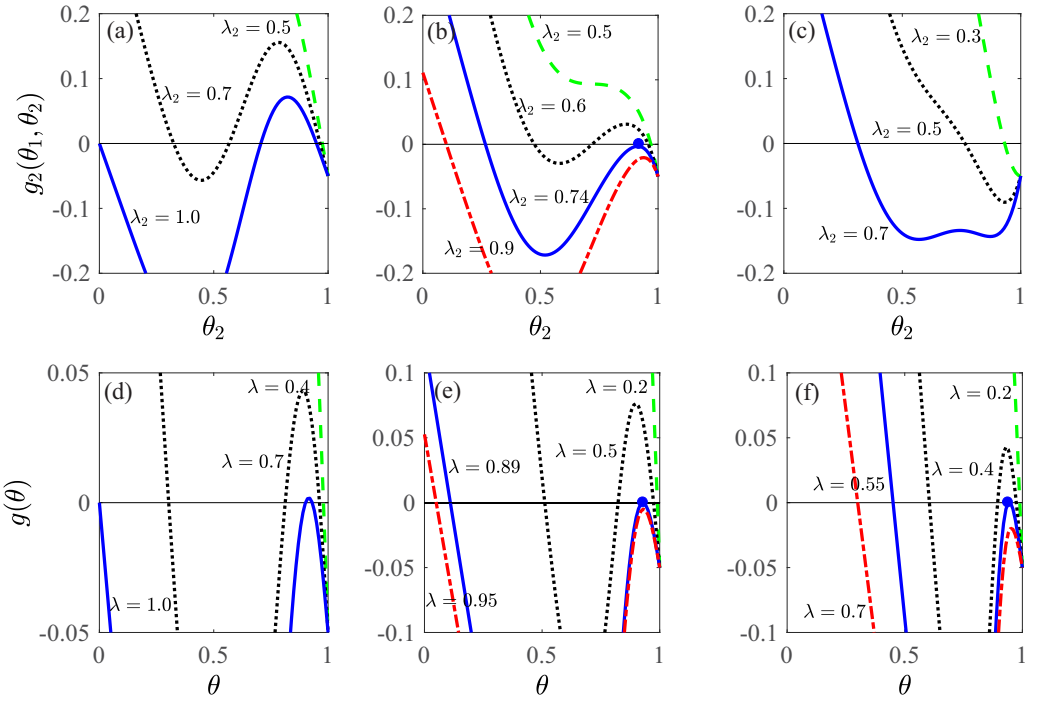

FIG. 2. Phase transitions associated with simultaneous behavioral spreading on double-layer random regular networks. The graphical solutions of Eqs. (18), (19), and (24) are presented. The upper panels show the results for the case $T_1 < T_2$, i.e., $T_1 = 1$ and $T_2 = 4$, where $g_2(\theta_1,\theta_2)$ is plotted as a function of θ_2 for $\Delta T_2 = 0$ (a), $\Delta T_2 = 2$ (b), and $\Delta T_2 = 3$ (c). The fixed points of Eqs. (17) and (18) are the intersections between the respective curves and the horizontal axis. Other parameters are $\Delta T_1 = 0$, $\lambda_1 = 0.12$, and $\rho_1(0) = \rho_2(0) = 0.05$. The lower panels show the cases of $T_1 = T_2$ for $T_1 = T_2 = 3$, $\Delta T_1 = \Delta T_2 = \Delta T$, and $\lambda_1 = \lambda_2 = \lambda$, where the values of $g(\theta)$ are plotted as a function of θ for $\Delta T = 0$ (d), $\Delta T = 1$ (e), and $\Delta T = 2$ (f). The fixed points of Eq. (24) are the intersections between the respective curves and the horizontal axis. The initial adoption fraction is $\rho(0) = 0.05$. The blue dots in (b), (e), and (f) denote the points of tangency. Other parameters are $\gamma_1 = \gamma_2 = 1$.

Because of the nonlinear functions $\Phi_1(k'_a,\theta_1,\theta_2)$ in Eq. (20) and $\Phi_2(k'_a,\theta_1,\theta_2)$ in Eq. (21), to analyze the whole parameter space is infeasible. We thus focus on some representative or benchmark cases to gain certain analytic understanding of the numerical results. Specifically, we consider two cases in terms of the adoption thresholds of the two behaviors: (1) the adoption threshold of one behavior is less than that of the other behavior ($T_1 < T_2$ or $T_1 > T_2$), and (2) $T_1 = T_2$.

B. Solutions for $T_1 < T_2$

For $T_1 < T_2$, $\Delta T_1 = 0$ and $\Delta T_2 > 0$, indicating that the adoption of behavior 2 has no effect on the spread of behavior 1 but the adoption of the latter will enhance the spread of former, as shown in Fig. 1. Because Eqs. (18) and (19) are nonlinear functions of θ_1 and θ_2, typically there are multiple roots. In addition, there is persistent transmission of behavioral information from individuals in an adopted state (i.e., A_1 or A_2) to their neighbors, so $\theta_1(t)$ and $\theta_2(t)$ decrease with time. Thus, if Eqs. (18) and (19) possess more than one stable fixed point, only the one with the maximum value is physically meaningful [30]. Since Eq. (18) contains the parameters λ_1 and θ_1 only, for a given value of λ_1, we can obtain the value of θ_1. For given values of the parameters λ_2 and ΔT_2, with θ_1 we can solve Eq. (19) numerically. As shown in the top panel of Fig. 2, we see that Eq. (19) typically has a nonzero trivial solution even for small values of λ_2, indicating that, even when the initial adopted fraction of behavior 2 is small [e.g., $\rho_2(0) = 0.05$], it will always be adopted by a certain fraction of the nodes. However, the initial fraction of seeds will have an effect on the final adoption size [17,30]. To better focus on the effect of synergistic interactions on simultaneous spreading of the two behaviors, we set $\rho_1(0) = \rho_2(0) = 0.05$ and calculate the final adoption size versus the behavioral information transmission rate with a particular eye on the possible type of phase transitions.

For $\Delta T_2 = 0$, the number of roots (fixed points) of the function $g_2(\theta_1,\theta_2) = f_2(\theta_1,\theta_2) - \theta_2$ is 1 or 3, as shown in Fig. 2(a). Because the physically meaningful solution is the maximum value of the stable fixed point of Eq. (19), there is no global outbreak in behavior 2 [verified numerically; see Fig. 4(a)]. For $\Delta T_2 = 2$, the function $g_2(\theta_1,\theta_2)$ is tangent to the horizontal axis at θ_2^c for the critical value of $\lambda_2^c \approx 0.74$. Further increasing λ_2 above λ_2^c removes the tangent point and leaves $g_2(\theta_1,\theta_2)$ with only one intersection point with the horizontal axis. Importantly, from the standpoint of bifurcation analysis, we see that, at this point, the physically meaningful fixed point θ_2 decreases abruptly to a small value, signifying a first-order phase transition. The critical value λ_2^c for a given λ_1 can be obtained by using the criterion that a nontrivial solution of Eq. (19) emerges, which corresponds to the point at which the function $g_2(\theta_1,\theta_2)$ is tangent to the horizontal axis at the critical value of θ_2^c. That is, the critical condition for this case can be obtained by combining Eqs. (18) and (19) and the following equation:

$$\left.\frac{dg_2(\theta_1,\theta_2)}{d\theta_2}\right|_{\theta_2^c} = 0. \tag{22}$$

For $\Delta T_2 = 3$ and $\lambda_1 = 0.12$, Eq. (19) has a single root whose value decreases with λ_2, as shown in Fig. 2(c). This means that $R_2(\infty)$ increases with λ_2 continuously.

For a given value of the transmission rate λ_1 of behavior 1, the critical condition is then that behavior 2 will be adopted if its transmission rate λ_2 is larger than λ_2^c. Similarly, we can compute the minimal information transmission rate of behavior 1 required for a global outbreak of behavior 2. In particular, setting λ_2 to be the maximum value (i.e., $\lambda_2 = 1.0$) and substituting it into Eqs. (19) and (22), we get the critical values of θ_1 and θ_2. Substituting these values into Eq. (18), we obtain λ_1^m, the minimal information transmission rate of behavior 1.

Numerical solutions of Eq. (19) also show that, for large values of λ_1 and $\Delta T_2 > 0$, it has one fixed point only when varying λ_2, so $R_2(\infty)$ increases with λ_2 continuously. As a result, there exists the critical parameter value θ_1^c (i.e., λ_1^c), across which the dependence of $R_2(\infty)$ on λ_2 changes from being discontinuous to continuous. For the special case of $T_1 < T_2$ (e.g., $T_1 = 1$, $T_2 = 4$, $\Delta T_1 = 0$, and $\Delta T_2 > 0$), we can numerically solve Eqs. (19) and (22), together with the condition [49]

$$\left.\frac{d^2 g_2(\theta_1,\theta_2)}{d\theta_2^2}\right|_{\theta_2^c} = 0. \tag{23}$$

Once θ_1^c is determined, we can substitute the value of θ_1^c into Eq. (18) to get λ_1^c. In particular, $R_2(\infty)$ increases with λ_2 discontinuously for $\lambda_1 < \lambda_1^c$ and the increasing pattern becomes continuous for $\lambda_1 \geqslant \lambda_1^c$. Using the same approach, we can determine the critical value of λ_2^c above (below) which $R_2(\infty)$ increases with λ_1 discontinuously (continuously).

C. Solutions for $T_1 = T_2$

This is the symmetric case where $\Delta T_1 = \Delta T_2 = \Delta T$, $\lambda_1 = \lambda_2 = \lambda$, $\langle k_a \rangle = \langle k_b \rangle$, and $P_a(k) = P_b(k) = P(k)$. The symmetry implies $\theta_1(t) = \theta_2(t)$ and $f_1(\theta_1,\theta_2) = f_2(\theta_1,\theta_2)$. For simplicity, we denote $\theta(t) \equiv \theta_1(t)$ and $f[\theta(t)] \equiv f_1[\theta_1(t),\theta_2(t)]$. Equations (18)–(21) can be written as

$$\theta = f(\theta), \tag{24}$$

where

$$f(\theta) = \frac{[1-\rho(0)]\sum_k kP(k)\Phi(k,\theta)}{\langle k \rangle} + \frac{\gamma}{\lambda}(1-\theta)(1-\lambda).$$

Similar to treating Eq. (8), we have

$$\Phi(k,\theta) = S(\infty)\sum_{m=0}^{T-1} B_{k-1,m}(\theta) + [1-S(\infty)]\sum_{m=0}^{T-1-\Delta T} B_{k-1,m}(\theta). \tag{25}$$

The final fraction of the susceptible nodes of behavior 1 (2) in layer a (b) is given by

$$S(\infty) = [1-\rho(0)]\sum_k P(k)\left\{S(\infty)\sum_{m=0}^{T-1} B_{k,m}(\theta) + [1-S(\infty)]\sum_{m=0}^{T-1-\Delta T} B_{k,m}(\theta)\right\}. \tag{26}$$

Using the same analysis method as for the case $T_1 < T_2$, we find that the number of fixed points of Eq. (24) is 1 or 3, as shown in the lower panel of Fig. 2. Whether there is a tangent point between the function $g(\theta) = f(\theta) - \theta$ and the horizon axis depends on the strength ΔT of synergistic interactions. For $\Delta T = 0$, there is no tangent point and only the maximum value of the fixed point of Eq. (24) is physically meaningful, indicating that behavior 2 is adopted by a small fraction of nodes only. For $\Delta T = 1$ and $\Delta T = 2$, the function $g(\theta)$ can be tangent to the horizon axis, as shown in Figs. 2(e) and 2(f). When λ_2 is increased passing through λ_2^c, the tangent point disappears and the function $g(\theta)$ has only one intersecting point with the horizontal axis. In this case, the fixed point θ changes discontinuously to a small value, signifying a first-order phase transition.

IV. NUMERICAL VALIDATION

In this section, we perform extensive simulations of behavior spreading on different multiplex networks. We use the notation "RR-RR" to denote the case where both layer a and layer b host the random regular networks. The notation "ER-SF" represents the setting where layer a is an Erdös-Rényi (ER) random network [50] and layer b hosts a scale-free (SF) network [51]. Other possible combinations are "ER-ER," "SF-SF," and "SF-ER." The size of each network is $N_a = N_b = 5 \times 10^4$ and the average degree is $\langle k \rangle = 10$ for both networks. The initial adoption fractions of behavior 1 in layer a and behavior 2 in layer b are set to be $\rho_1(0) = \rho_2(0) = 0.05$. To calculate the pertinent statistical averages, we use 20 multiplex network realizations and at least 10^3 independent dynamical realizations for each parameter setting. Unless otherwise specified, the above parameters are adopted in the simulations. Let X_1 denote the situation where a node is in the A or R state in layer a so, for example, the notion X_1S_2 means that, in layer a, a node is in the adopted state or recovered state but it is in the susceptible state in layer b. Similarly, A_1S_2 indicates that a node is in the adopted state in layer a and is in the susceptible state in layer b, which means that the node adopts behavior 1 but not behavior 2.

A. RR-RR multiplex networks

We first perform direct numerical simulations of behavioral spreading dynamics on double layer networked systems consisting of two random regular networks to provide support for our theoretical predictions.

Our theoretical analysis in Sec. III B gives that, for $T_1 < T_2$, synergistic interactions can promote behavior adoption and spreading. To be concrete, we set $T_1 = 1$ and $T_2 = 4$. Figure 3(a) shows the time evolution of the fraction $R_2(t)$ of the recovered nodes in layer b for different values of the synergistic interaction strength ΔT_2. We see that behavior 2 will not break out if $\Delta T_2 = 0$. For $\Delta T_2 = 2$ and $\Delta T_2 = 3$, $R_2(t)$ exhibits a two-stage contagion process, where nodes having adopted behavior 1 in layer a will first adopt behavior 2, until when there is a sufficient number of seeds (i.e., nodes having adopted behavior 2) in layer b to stimulate the remaining nodes. When this happens, behavior 2 will be adopted quickly in layer b. This phenomenon can be explained by noting that,

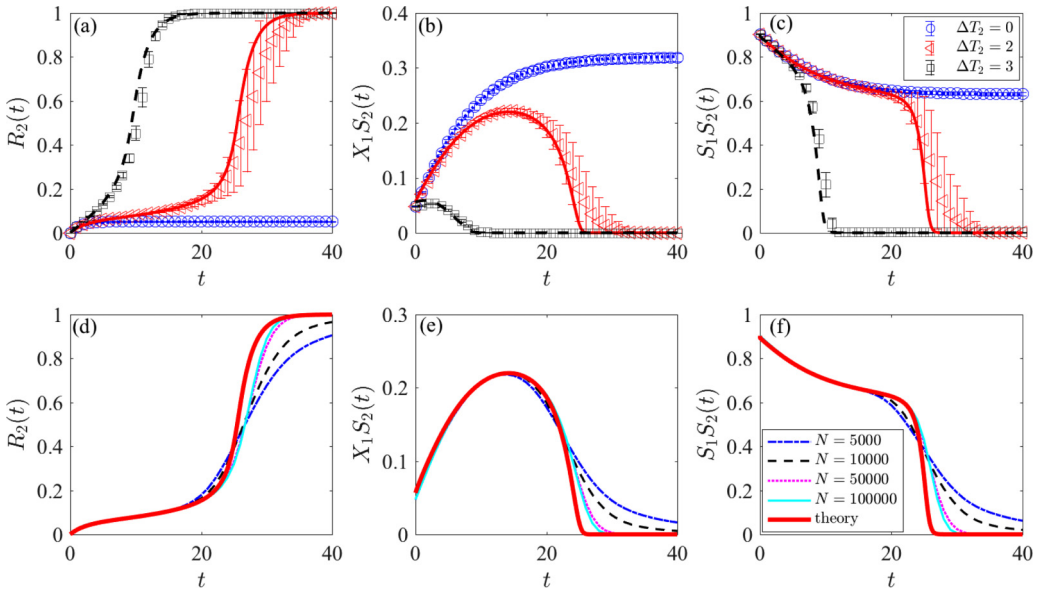

FIG. 3. Time evolution of behavior spreading subject to synergistic interactions. For random regular double-layer networks, (a),(d) the fraction of recovered nodes $R_2(t)$ versus time t, (b),(e) the fraction of nodes in state X in layer a and in state S in layer b versus time, (c),(f) the fraction of nodes in the S state in both layers a and b versus time. (d)–(f) are the simulation results when $\Delta T_2 = 2$ for different network sizes N. The parameters are $\lambda_1 = 0.06$, $\lambda_2 = 0.8$, $T_1 = 1$, $T_2 = 4$, and $\Delta T_1 = 0$. The symbols are simulation results and the lines are theoretical prediction in (a)–(c). In the theoretical analysis of the state $X_1S_2(t)$, dynamical correlations between the layers are ignored. Other parameters are $\gamma_1 = \gamma_2 = 0.5$.

for a small fraction of the initial seeds for behavior 2 [i.e., $\rho_2(0) = 0.05$], if the synergistic effect of adoption of behavior 1 is absent (i.e., $\Delta T_2 = 0$), behavior 2 will not be adopted globally and only the recovery of the seeds can lead to an increase in the value of $R_2(t)$. Note that the number of $X_1S_2(t)$ nodes increases with the adoption of behavior 1 in layer a [Fig. 3(b)] since the S_1 nodes will change to X_1 nodes and there is no decrease in the number of S_2 nodes in the network. For $\Delta T_2 = 2$, nodes that have adopted behavior 1 are more likely to adopt behavior 2 as compared with those that have not adopted behavior 1. Nodes having adopted behavior 1 in layer a will first adopt behavior 2 in layer b, as indicated by the decrease in the number of the $X_1S_1(t)$ nodes in Fig. 3(c). Before most of the X_1S_2 nodes have adopted behavior 2, the seeds (i.e., adopted nodes for behavior 2) in layer b are sufficient to stimulate the remaining nodes to adopt behavior 2, inducing a two-stage contagion process. A similar phenomenon occurs for $\Delta T_2 = 3$. When the simulation results are compared with the theoretical predictions, we find the former matches well with the latter for $\Delta T_2 = 0$, while the deviation emerges when $\Delta T_2 = 2$, which is derived from the finite-size effects of the networks and the dynamical correlation between layers. From the bottom panels of Fig. 3, we will find that the deviation is decreased when increasing the network size, but the deviation will still exist since the interlayer dynamical correlations are ignored in the theoretical method.

Figure 4(a) shows, for $T_1 = 1$, $T_2 = 4$, and $\lambda_1 = 0.12$, $R_2(\infty)$ versus λ_2 for different values of ΔT_2, where the fraction of the X_1S_2 nodes in the system is about 0.393. As the synergistic interaction strength ΔT_2 is increased, behavior 2 is adopted more readily since the number of information pieces about it is decreased. A remarkable phenomenon is the characteristic change in the dependence of $R_2(\infty)$ on λ_2. In particular, for $\Delta T_2 = 2$, $R_2(\infty)$ increases with λ_2 discontinuously but the increasing pattern becomes continuous for $\Delta T_2 = 3$. The reason for the characteristic change is that, for $\Delta T_2 = 2$, the nodes having adopted behavior 1 still need to receive an additional *two* (i.e., $T_2 - \Delta T_2$) pieces of information to adopt behavior 2. The system will accumulate a relatively large number of nodes in the subcritical state when the behavioral information transmission rate approaches the critical point, as shown in the inset of Fig. 4(a). Therein, the subcritical state is defined that the node in such state will adopt the behavior if it receives one additional piece of behavior information [30]. A slight increase in λ_2 will cause a node in this state to receive an additional piece of information and thus adopts behavior 2. The node can then transmit the information to its neighbors, which will cause its subcritical neighbors to adopt behavior 2 accordingly, and so on, leading to an avalanche of behavior adoption for the X_1S_2 nodes. When most of the X_1S_2 nodes have adopted behavior 2 in an abrupt fashion, there is a sufficient number of A_2 nodes in layer b to stimulate the remaining S_1S_2 nodes to adopt behavior 2. As a result, increasing λ_2 slightly can lead to a discontinuous change in the value of $R_2(\infty)$. However, for $\Delta T_2 = 3$, only one additional piece of information about behavior 2 is needed for the X_1S_2 nodes to adopt this behavior. As the value of λ_2 is increased from zero, some X_1S_2 nodes may receive one piece of information about behavior 2 and adopt it, leading to a continuous decrease in the number of nodes in the subcritical state, as shown in the inset of Fig. 4(b). This is equivalent to the dynamical process in the susceptible-infected-recovered (SIR) model, in contrast to the cascading process in, for example, the Watts threshold model. As a result, the value of $R_2(\infty)$ first increases with λ_2 continuously. When most of the X_1S_2 nodes have adopted behavior 2, the fraction of adopted nodes

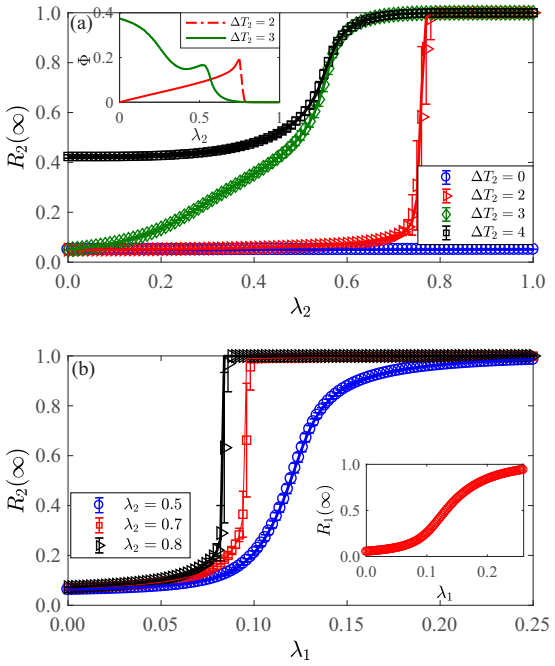

FIG. 4. Asymptotic and stable adoption of behavior 2. For random regular double-layer networks, the final adoption size of behavior 2 versus the information transmission rates: (a) $R_2(\infty)$ versus λ_2 for different values of the synergistic strength ΔT_2, where the transmission rate for behavior 1 is $\lambda_1 = 0.12$ and the corresponding fraction of the nodes adopting behavior 1 is $R_1(\infty) \approx 0.393$, (b) $R_2(\infty)$ versus λ_1 for different values of λ_2. The inset in (a) shows the final fraction Φ of nodes in the subcritical state for behavior 2. The subcritical state is defined as the state for a node that it will adopt the behavior when it receives one additional piece of information. The inset in (b) shows the final adoption fraction of behavior 1 in layer a versus λ_1, where $\Delta T_2 = 3$. The symbols are simulation results and the lines (i.e., dotted, dotted dashed, and solid lines) are theoretical prediction. Other parameters are $T_1 = 1, T_2 = 4, \Delta T_1 = 0$, and $\gamma_1 = \gamma_2 = 1$.

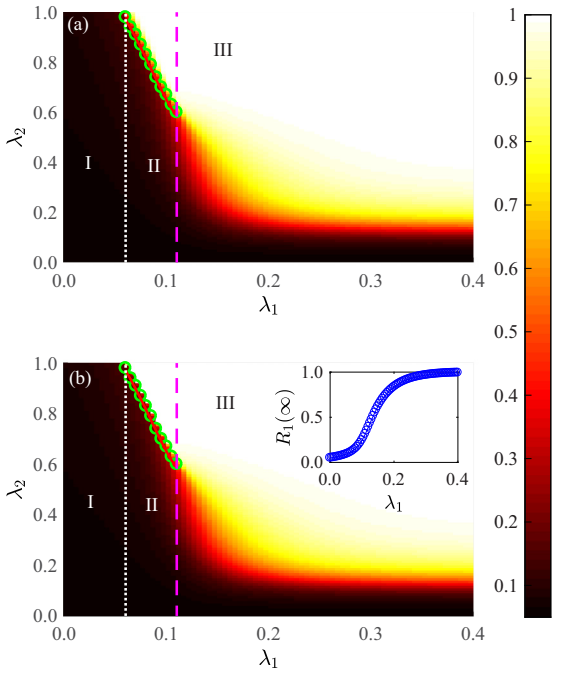

FIG. 5. Dependence of final adoption size of behavior 2 on the transmission rates. For random regular networks, color coded values of $R_2(\infty)$ in the parameter plane (λ_1, λ_2) of the two information transmission rates: (a) numerical results and (b) theoretical prediction based on solutions of Eqs. (1)–(4) and (16)–(19). The plane is divided into three regions by the two vertical lines, where the dotted vertical line $(\lambda_1 = \lambda_1^m)$ is from Eqs. (18), (19), and (22) for $\lambda_2 = 1$, and the dashed vertical line $(\lambda_1 = \lambda_1^c)$ is determined by Eqs. (18), (19), (22), and (23). In region I, only a small fraction of the nodes is exposed to adopting behavior 2. In regions II and III, there is a discontinuous (first-order) and a continuous (second-order) phase transition, respectively. The green circles and the red line in region II, respectively, indicate the numerically obtained critical information transmission rate of behavior 2 and the theoretical prediction from Eqs. (17), (19), and (22) for a given value of λ_1. The inset in (b) shows the final adoption fraction of behavior 1 versus the information transmission rate of this behavior. Other parameters are $T_1 = 1$, $\Delta T_1 = 0$, $T_2 = 4$, $\Delta T_2 = 3$, and $\gamma_1 = \gamma_2 = 1$.

in layer b is sufficient to stimulate the remaining $S_1 S_2$ nodes to adopt behavior 2. Since the fraction of adopted nodes is relatively large [e.g., $X_1(\infty) \approx 0.393$], the value of $R_2(\infty)$ increases with λ_2 continuously [30] at a faster rate, as shown in Fig. 4(a). The same process occurs for $\Delta T_2 = 4$. These numerical results agree well with our bifurcation analysis based theoretical prediction.

Figure 4(b) shows the dependence of $R_2(\infty)$ on λ_1 for different values of λ_2. For a relatively small value of λ_2 (e.g., $\lambda_2 = 0.5$), $R_2(\infty)$ increases with λ_1 continuously, which can be understood by noting that, in this case, a global adoption of behavior 2 requires more seeds in layer b, and the spread of this behavior depends strongly on the spread of behavior 1. However, for relatively large values of λ_2 (e.g., $\lambda_2 = 0.7$ and $\lambda_2 = 0.8$), $R_2(\infty)$ versus λ_1 can exhibit an abrupt or discontinuous increase. In this case, a slight increase in the fraction of seeds for behavior 2 is sufficient for it to spread globally by its own dynamics. Both the continuous growth for small values of λ_2 and the discontinuous increase for larger values of λ_2 are predicted by our bifurcation analysis based on Eqs. (18), (19), (22), and (23) by replacing θ_2 with θ_1 in Eqs. (22) and (23). There is a good agreement between numerics and theory.

Our analysis and numerical computations indicate that, with synergistic interactions between the spreading dynamics of two behaviors, both λ_1 and λ_2 can affect $R_2(\infty)$ and the associated phase transition characteristically. To further demonstrate the role of the synergistic interactions, we show in Fig. 5 color coded values of $R_2(\infty)$ in the parameter plane (λ_1, λ_2) for $T_1 = 1$, $T_2 = 4$, $\Delta T_1 = 0$, and $\Delta T_2 = 3$. There are three regions in the parameter plane, determined by the two vertical lines at λ_1^m and λ_1^c, respectively, which are associated with characteristically distinct behavioral adoption dynamics. In region I $(\lambda_1 < \lambda_1^m)$, only a small fraction of the nodes in layer b adopt behavior 2. In region II $(\lambda_1^m < \lambda_1 \leqslant \lambda_1^c)$, there is a discontinuous phase transition, where a larger fraction of nodes adopt behavior 2 for $\lambda_2 > \lambda_2^c$ (white solid line). In region III $(\lambda_1 > \lambda_1^c)$, there is a continuous phase transition. The distinct

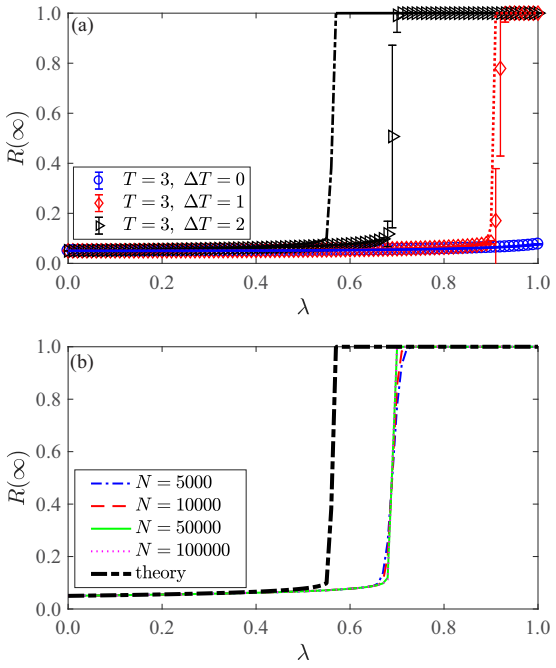

FIG. 6. Behavioral adoption dynamics under symmetrical synergistic interactions. For random regular double-layer networks, (a) the fraction of recovered nodes $R(\infty)$ [i.e., $R_1(\infty) = R_2(\infty) \equiv R(\infty)$] versus λ, where $\lambda_1 = \lambda_2 \equiv \lambda$. The symbols are simulation results and the solid lines are the theoretical prediction obtained by iterating Eqs. (24) and (26). (b) The simulation results of $R(\infty)$ versus λ when $T = 3$ and $\Delta T = 2$ for different network sizes N. Other parameters are $\gamma_1 = \gamma_2 = 1$.

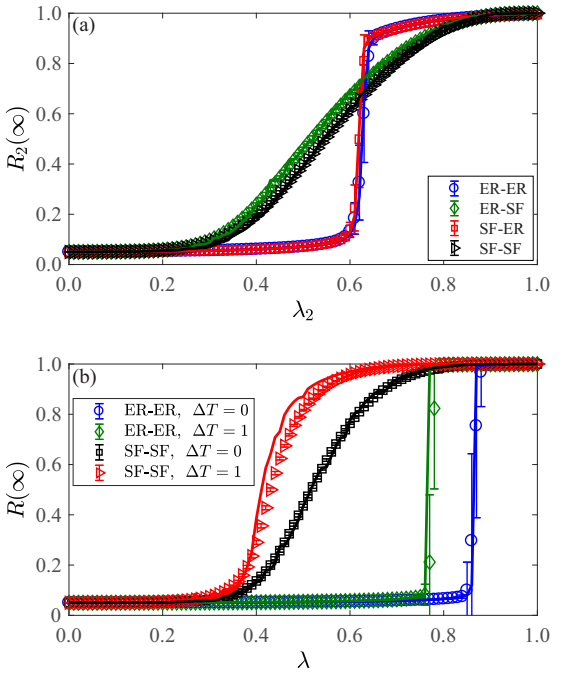

FIG. 7. Synergistic behavior spreading on a multiplex networked system with heterogeneous network layers. For $T_1 < T_2$, (a) $R_2(\infty)$ versus λ_2, where $T_1 = 1$, $T_2 = 4$, $\Delta T_1 = 0$, and $\Delta T_2 = 2$. (b) The fraction of recovered nodes $R(\infty)$ versus λ. The parameters are $T_1 = T_2 = 3$, $\Delta T_1 = \Delta T_2 = \Delta T$, $\lambda_1 = \lambda_2 = \lambda$, and $R_1(\infty) = R_2(\infty) = R(\infty)$. The symbols are simulation results and the solid lines are theoretical prediction. Other parameters are $\gamma_1 = \gamma_2 = 1$.

types of phase transition are predicted through our bifurcation analysis in Sec. III.

To gain further insight into the effects of synergistic interactions in behavioral adoption dynamics, we study the special case where the two types of behaviors are completely symmetric to each other. Figure 6(a) shows, for $T_1 = T_2 = T$, $\Delta T_1 = \Delta T_2 \equiv \Delta T$, and $\lambda_1 = \lambda_2 \equiv \lambda$, the dependence of $R(\infty)$ on λ for different values of ΔT. In the absence of synergistic interactions, i.e., when the adoptions of behaviors 1 and 2 have no effect on each other, neither behavior can spread globally and either behavior can only be adopted by a small fraction of the nodes in the network. For $\Delta T > 0$ (i.e., $\Delta T = 1,2$), the nodes that have adopted behavior 1 (2) only need additional $T - \Delta T$ pieces of information to adopt behavior 2 (1). As a result, the mutually cooperative spreading of behaviors 1 and 2 leads to a wide adoption of both behaviors. Increasing the synergistic interaction strength makes the dynamical correlation between the two layers stronger. The discontinuous phase is more clear when the network size is enlarged. However, the improvement in decreasing the deviation of the critical threshold is less, as shown in Fig. 6(b). In this regime, the deviation is mainly because the theoretical method cannot capture the strong dynamical correlation between layers.

B. General multiplex networks

We consider more general network topology for the network layers in the multiplex system, such as ER-ER, SF-SF, ER-SF, and SF-ER. We use the standard configuration model [45] to construct SF networks with the degree distribution $P(k) = \Gamma k^{-\gamma}$, where $\gamma = 3$ is the degree exponent and the coefficient is $\Gamma = 1/\sum_{k_{\min}}^{k_{\max}} k^{-\gamma}$ with the minimum degree $k_{\min} = 3$ and maximum degree $k_{\max} \sim N^{1/(\gamma-1)}$. The average degrees of SF and ER networks are set as $\langle k \rangle = 10$, and the network size is $N = 5 \times 10^4$. For $T_1 < T_2$, e.g., $T_1 = 1$ and $T_2 = 4$, we fix the final adoption size of behavior 1 and vary the type of network in layer a.

To facilitate comparison, we set $\lambda_1 = 0.12$ when layer a is an ER network and $\lambda_1 = 0.113$ if network a is SF, so that the final adoption sizes of behavior 1 for both cases are approximately 0.44. As shown in Fig. 7(a), the network type in layer a over which behavior 1 spreads has little effect on the spread of behavior 2. For the symmetric case $T_1 = T_2$, the dependence of $R(\infty)$ on λ changes from being discontinuous to continuous as the network becomes more heterogeneous (i.e., SF) [30], as a strong heterogeneity makes it harder for nodes in the subcritical state to adopt a behavior simultaneously. Regardless of the network type, in general synergistic interactions can facilitate adoption of both behaviors and alter the nature of the associated phase transition.

V. DISCUSSION

To understand social contagions in the human society at a quantitative level is of great importance in the modern time. While the spread of a single contagion can be analyzed through the traditional models of network spreading dynamics,

the simultaneous presence and spreading of two or more contagions poses a challenge due to the mutual interplay between the underlying dynamical processes. As an initial effort to address this problem, we articulate a spreading model of multiple social behaviors on multiplex networks subject to synergistic interactions. For simplicity, we consider two-layer coupled networks and limit the number of distinct behaviors to two: one on each layer. The manifestation of the synergistic mechanism is that the adoption of the behavior by a node in one layer will increase the chance for the node that is simultaneously present in the other layer to adopt the behavior that spreads in that layer. The concrete setting enables us to develop an edge-based compartmental theory and a bifurcation analysis to uncover and explain how the synergistic interactions affects the spreading dynamics in terms of the final adoption size and the distinct phase transitions.

There are two types of synergistic interactions: asymmetric and symmetric. In the asymmetric case, the adoption threshold of one behavior in one network layer is less than that of the other behavior in the other layer. In this case, the adoption of the behavior with the higher threshold has no effect on the adoption of the other behavior. However, synergistic interactions can promote the adoption of both behaviors. In fact, the interaction strength and the information transmission rate of the behavior with the smaller threshold value can affect the nature of the phase transition of the behavior with the larger threshold: a small (large) value of the transmission rate of the former can lead to a discontinuous (continuous), first- (second-)order phase transition in the latter. In addition, a two stage spreading process arises: nodes adopting the small threshold behavior in one layer are more likely to adopt the large threshold behavior in the other layer, which stimulates the remaining nodes in this layer to quickly adopt the behavior. In the case of symmetric synergistic interactions, the adoption processes in both layers can affect each other on an equal footing. In this case, the interactions will greatly enhance the spreading of both behaviors in their respective layers through a first-order phase transition.

Many issues remain, such as the effect of heterogeneity in the synergistic strengths of the individual nodes on behavioral spreading and the impacts of degree correlation between the network layers. In general, there are two kinds of dynamical correlation: intralayer and interlayer. In each layer, the correlation can be described by the edge-based compartmental theory. To make a theoretical analysis feasible, we have neglected interlayer correlation, i.e., the dynamical correlation among nodes in distinct layers. However, in real situations, dynamical correlation may exist between the same node in different layers, depending on the strength of the synergistic interaction. If the interaction strength is not too large, interlayer dynamical correlation is weak. In this case, there is a good agreement between the theoretical prediction and the simulation results (e.g., Figs. 1 and 4). For relatively strong synergistic interaction (e.g., Fig. 6 for $\Delta T = 2$), the simulation results deviate from the theoretical prediction. Increasing the size of network will not help reduce the deviation, as interlayer correlation can no longer be regarded as insignificant. A more accurate theory incorporating interlayer correlation is thus needed for synergistic affected information spreading in the strong interaction regime [52].

ACKNOWLEDGMENTS

We are very grateful for the comments of anonymous reviewers. We thank A. Vespignani and Q. Zhang at the Laboratory for Modeling of Biological Socio-technical Systems (MOBS LAB) for valuable discussions and comments. This work was supported by the National Natural Science Foundation of China under Grants No. 11575041 and No. 61673086, the program of China Scholarships Council, and the Fundamental Research Funds for the Central Universities (Grant No. ZYGX2015J153). Y.C.L. would like to acknowledge support from the Vannevar Bush Faculty Fellowship program sponsored by the Basic Research Office of the Assistant Secretary of Defense for Research and Engineering and funded by the Office of Naval Research through Grant No. N00014-16-1-2828.

[1] A. Barrat, M. Barthélemy, and A. Vespignani, *Dynamical Processes on Complex Networks* (Cambridge University Press, Cambridge, UK, 2008).
[2] A. Vespignani, Nat. Phys. **8**, 32 (2012).
[3] R. Pastor-Satorras, C. Castellano, P. Van Mieghem, and A. Vespignani, Rev. Mod. Phys. **87**, 925 (2015).
[4] T. W. Valente, Soc. Net. **18**, 69 (1996).
[5] N. A. Christakis and J. H. Fowler, New Eng. J. Med. **357**, 370 (2007).
[6] H. P. Young, Am. Econ. Rev. **99**, 1899 (2009).
[7] E. M. Rogers, *Diffusion of Innovations* (Simon and Schuster, New York, 2010).
[8] D. Centola, Science **334**, 1269 (2011).
[9] A. Banerjee, A. G. Chandrasekhar, E. Duflo, and M. O. Jackson, Science **341**, 1236498 (2013).
[10] Y. Zha, T. Zhou, and C. Zhou, Proc. Natl. Acad. Sci. USA **113**, 14627 (2016).
[11] Z.-K. Zhang, C. Liu, X.-X. Zhan, X. Lu, C.-X. Zhang, and Y.-C. Zhang, Phys. Rep. **651**, 1 (2016).
[12] C. Castellano, S. Fortunato, and V. Loreto, Rev. Mod. Phys. **81**, 591 (2009).
[13] P. S. Dodds and D. J. Watts, Phys. Rev. Lett. **92**, 218701 (2004).
[14] P. S. Dodds and D. J. Watts, J. Theor. Biol. **232**, 587 (2005).
[15] M. S. Granovetter, Am. J. Soc. **78**, 1360 (1973).
[16] D. J. Watts, Proc. Natl. Acad. Sci. USA **99**, 5766 (2002).
[17] J. P. Gleeson and D. J. Cahalane, Phys. Rev. E **75**, 056103 (2007).
[18] D. E. Whitney, Phys. Rev. E **82**, 066110 (2010).
[19] A. Hackett, S. Melnik, and J. P. Gleeson, Phys. Rev. E **83**, 056107 (2011).
[20] Y. Zhuang, A. Arenas, and O. Yağan, Phys. Rev. E **95**, 012312 (2017).
[21] J. P. Gleeson, Phys. Rev. E **77**, 046117 (2008).
[22] A. Nematzadeh, E. Ferrara, A. Flammini, and Y.-Y. Ahn, Phys. Rev. Lett. **113**, 088701 (2014).

[23] C. D. Brummitt, K.-M. Lee, and K.-I. Goh, Phys. Rev. E **85**, 045102 (2012).
[24] O. Yağan and V. Gligor, Phys. Rev. E **86**, 036103 (2012).
[25] E. Cozzo, R. A. Banos, S. Meloni, and Y. Moreno, Phys. Rev. E **88**, 050801 (2013).
[26] D. Centola, Science **329**, 1194 (2010).
[27] P. L. Krapivsky, S. Redner, and D. Volovik, J. Stat. Mech. Theor. Exp. (2011) P12003.
[28] M. Zheng, L. Lü, and M. Zhao, Phys. Rev. E **88**, 012818 (2013).
[29] Q.-H. Liu, W. Wang, M. Tang, and H.-F. Zhang, Sci. Rep. **6**, 25617 (2016).
[30] W. Wang, M. Tang, H.-F. Zhang, and Y.-C. Lai, Phys. Rev. E **92**, 012820 (2015).
[31] W. Wang, M. Tang, P. Shu, and Z. Wang, New J. Phys. **18**, 013029 (2016).
[32] W. Wang, P. Shu, Y.-X. Zhu, M. Tang, and Y.-C. Zhang, Chaos **25**, 103102 (2015).
[33] M.-X. Liu, W. Wang, Y. Liu, M. Tang, S.-M. Cai, and H.-F. Zhang, Phys. Rev. E **95**, 052306 (2017).
[34] Q.-H. Liu, W. Wang, M. Tang, T. Zhou, and Y.-C. Lai, Phys. Rev. E **95**, 042320 (2017).
[35] S. A. Myers and J. Leskovec, in *Proceedings of the IEEE 12th International Conference on Data Mining (ICDM), Brussels, Belgium* (IEEE, 2012), pp. 539–548.
[36] A. Zarezade, A. Khodadadi, M. Farajtabar, H. R. Rabiee, and H. Zha, in *Proceedings of the 31st AAAI Conference on Artificial Intelligence* (AAAI, Phoenix, 2016), pp. 238–244.
[37] J. Taubenberger and D. Morens, Emerg. Infect. Dis. **12**, 15 (2006).
[38] J. F. Brundage and G. Shanks, Emerg. Infect. Dis. **14**, 1193 (2008).
[39] L. Chen, F. Ghanbarnejad, W. Cai, and P. Grassberger, Europhys. Lett. **104**, 50001 (2013).
[40] W. Cai, L. Chen, F. Ghanbarnejad, and P. Grassberger, Nat. Phys. **11**, 936 (2015).
[41] L. Hébert-Dufresne and B. M. Althouse, Proc. Natl. Acad. Sci. USA **112**, 10551 (2015).
[42] M. D. Domenico, C. Granell, M. A. Porter, and A. Arenas, Nat. Phys. **12**, 901 (2016).
[43] M. Kivelä, A. Arenas, M. Barthelemy, J. P. Gleeson, Y. Moreno, and M. A. Porter, J. Complex Net. **2**, 203 (2014).
[44] S. Boccaletti, G. Bianconi, R. Criado, C. I. Del Genio, J. Gómez-Gardenes, M. Romance, I. Sendina-Nadal, Z. Wang, and M. Zanin, Phys. Rep. **544**, 1 (2014).
[45] M. Catanzaro, M. Boguñá, and R. Pastor-Satorras, Phys. Rev. E **71**, 027103 (2005).
[46] J. C. Miller, A. C. Slim, and E. M. Volz, J. R. Soc. Interface **9**, 890 (2012).
[47] Z. Yang and T. Zhou, Phys. Rev. E **85**, 056106 (2012).
[48] B. Karrer and M. E. J. Newman, Phys. Rev. E **82**, 016101 (2010).
[49] G. J. Baxter, S. N. Dorogovtsev, A. V. Goltsev, and J. F. F. Mendes, Phys. Rev. E **82**, 011103 (2010).
[50] P. Erdős and A. Rényi, Publ. Math. **6**, 290 (1959).
[51] A.-L. Barabási and R. Albert, Science **286**, 509 (1999).
[52] W. Wang, M. Tang, H. E. Stanley, and L. A. Braunstein, Rep. Prog. Phys. **80**, 036603 (2017).